Effect of Combined Particle-Phase Diffusivity and Viscosity on the Compressible Boundary Layer of a Particulate Suspension Over a Flat Plate

A. J. Chamkha
Department of Mechanical and Industrial Engineering,
Kuwait University,
Safat 13060, Kuwait

A mathematical dilute fluid-particle suspension model governing steady, laminar, compressible, boundary layer flow and heat transfer over a semi-infinite flat plate based on the Eulerian or continuum approach is developed. The model accounts for both particulate viscous and diffusive effects. Both the fluid and the particle phases are assumed to have general power-law viscosity-temperature relations. For the case of finite particle-phase viscosity, a general boundary condition borrowed from rarefied gas dynamics is used for the particle phase at the surface. Uniform and nonuniform particle-phase slip coefficients are investigated. Numerical solution of the governing equations is obtained by an implicit, iterative, tridiagonal finite difference method. Graphical results for the displacement thicknesses and skin-friction coefficients of both phases as well as the wall heat transfer are presented for various parametric conditions.

Introduction

Boundary layer flow and heat transfer of pure and contaminated fluids have been an attractive research area for many investigators for many years due to its direct application in the aerospace, automotive, petroleum, geothermal, and many other industries. There has been considerable work carried out on incompressible and compressible boundary layer flow of a fluid through and over many different geometries (see, for instance, Young, 1949; Kuerti, 1951; Stewartson, 1974). The presence of solid particles in fluid processes, such as gas purification, has led to the consideration and investigation of two-phase fluid-particle flow systems.

It has been shown by many previous investigators that the presence of a second phase (like solid particles) in the fluid with a relatively high level of concentration significantly alters the flow and heat transfer characteristics as well as adds complexity in obtaining a solution to the problem from both numerical and experimental points of view. The present paper considers a fundamental problem in two-phase flow. This problem is that of steady, laminar, compressible, boundary layer flow and heat transfer of a gas-particle suspension over a semi-infinite flat plate. The particle phase is assumed to consist of very tiny particles and exhibits a motion of Brownian type and has relatively high concentration to account for the particulate viscous effects. In addition, interparticle forces are neglected so that the system is dilute. This has possible applications in such processes as fluidized beds, gas purification, conveying of powdered materials and transport process, and environmental related problems such as dust storms. Special cases of the present problem have been considered earlier by Singleton (1965) and Wang and Glass (1988). Both of these references obtained asymptotic solutions using the series expansion method. In addition, Wang and Glass (1988) reported numerical solutions based on the finite-difference methodology. Recently, Chamkha (1996a) generalized the problem considered by Singleton (1965) and Wang and Glass (1988) for a relatively dense suspension for which particle-phase viscous effects are important. In another contribution, Chamkha (1996b) has also considered the case of finite particulate volume fraction where, a uniform particle-phase density distribution is predicted. Recently, Chamkha (1998) has investigated the influence of particle-phase diffusive effects which produced significant changes in the wall particle-phase density distribution and heat transfer.

A literature survey shows that extensive research investigations have been carried out on the incompressible version of the problem under consideration. Reviews of this work can be seen in the works of Soo (1968), Osiptsov (1980), Prabha and Jain (1982), Datta and Mishra (1982), Chamkha and Peddieson (1989, 1992), and Chamkha (1994). A major conclusion of the work on the incompressible problem is that when the original dusty-gas model (a model meant for the description of particulate suspension having small particulate volume fraction and excludes particulate viscous and diffusive effects) discussed by Marble (1970), a singular behavior in which the particle-phase density at the plate surface becomes infinite is predicted. In contrast with this conclusion, the work of Chamkha (1996a) has shown that for a compressible boundary layer flow of a dense particulate suspension, a particle-free zone is predicted somewhere downstream of the leading edge of the plate.

The presence of particle-phase diffusivity in the original dusty-gas model have shown to be capable of removing the singularity predicted in the incompressible problem (see Chamkha and Peddieson, 1989; Chamkha 1994). It is of interest in the present work to investigate whether the inclusion of particle-phase diffusive effects in the dusty-gas model will have the same influence on the compressible problem for both inviscid and viscous particle-phase conditions. Also, of interest is the study of the effects of both uniform and nonuniform particle-phase wall-slip conditions. The dynamic viscosities of both phases, the fluid-phase thermal conductivity and the particle-phase diffusivity are represented by general power-law functions of the fluid-phase temperature and the particle-phase temperature, respectively. The interaction between the phases is limited to drag and heat transfer. The particles are assumed to be very small and of spherical shape, and their volume fraction is assumed small.

Contributed by the Heat Transfer Division for publication in the JOURNAL OF HEAT TRANSFER. Manuscript received by the Heat Transfer Division, Oct. 7, 1998; revision received, Dec. 1, 1998. Keywords: Computational, Forced Convection, Heat Transfer, Laminar, Two-Phase. Associate Technical Editor: R. Douglass.

Governing Equations

Consider steady, compressible, laminar, boundary layer two-phase flow in a half-space bounded by a semi-infinite flat surface. The surface or plate is coincident with the plane $y = 0$ and the flow is a uniform stream in the plane $y > 0$ parallel to the surface. Far from the surface, both phases are in both hydrodynamic and thermal equilibrium. The particles are all assumed to be of one size and spherical in shape and moving with the same velocity. Radiative heat transfer from one particle to another, chemical reaction, coagulation, phase change, and deposition are all neglected. The fluid phase is assumed to behave as a perfect gas. The fluid and particles motions are coupled only through drag and heat transfer between them. The drag force is modeled using Stokes linear drag theory and the small particle volume fraction assumption inherent in the dusty-gas model (see Marble, 1970) is retained in this problem.

The governing equations for this investigation are based on the balance laws of mass, linear momentum, and energy for both phases. These can be written

$$\nabla \cdot (\rho \mathbf{V}) = S_f \tag{1a}$$

$$\nabla \cdot (\rho_p \mathbf{V}_p) = S_p \tag{1b}$$

$$\rho \mathbf{V} \cdot \nabla \mathbf{V} = \nabla \cdot \underline{\sigma} - \mathbf{f} \tag{1c}$$

$$\rho_p \mathbf{V}_p \nabla \cdot \mathbf{V}_p = \nabla \cdot \underline{\sigma}_p + \mathbf{f} \tag{1d}$$

$$\rho c \mathbf{V} \cdot \nabla T = \nabla \cdot (k \nabla T) + \underline{\sigma} : \nabla \mathbf{V} + (\mathbf{V} - \mathbf{V}_p) \cdot \mathbf{f} + Q_T \tag{1e}$$

$$\rho_p c_p \mathbf{V}_p \cdot \nabla T_p = \underline{\sigma}_p : \nabla \mathbf{V}_p - Q_T. \tag{1f}$$

The previous equations are supplemented by the following constitutive equations:

$$S_f = 0,\ S_p = D_p \nabla^2 \rho_p \tag{2a,b}$$

$$\underline{\sigma} = -P\underline{I} + \mu(T)(\nabla \mathbf{V} + \nabla \mathbf{V}^T) \tag{2c}$$

$$\underline{\sigma}_p = \mu_p(T_p)(\nabla \mathbf{V}_p + \nabla \mathbf{V}_p^T) \tag{2d}$$

$$\mathbf{f} = \rho_p(\mathbf{V} - \mathbf{V}_p)/\tau_v \tag{2e}$$

$$Q_T = \rho_p c_p (T_p - T)/\tau_T \tag{2f}$$

$$P = \rho R T. \tag{2g}$$

It is seen from Eqs. (2) that the particle phase is assumed to have diffusive and viscous effects which are not present in the models reported by Singleton (1965) and Wang and Glass (1988). It should be mentioned that Eq. (1*b*) for the particle phase is familiar from dynamics of chemically reacting flows. Also, the particle-phase diffusivity can be incorporated into the mathematical model through the particle-phase momentum equation. Since the present formulation has worked well for the incompressible version (see Chamkha and Peddieson, 1989) and for the sake of comparison, it is adopted herein. Particle-phase diffusivity is needed to model Brownian motion and is often employed to facilitate numerical solutions (see Chamkha and Peddieson, 1989; Chamkha, 1994). Particle-phase viscosity is often employed to model particle-particle interaction and particle-wall interaction. Theoretically, it can result from the averaging processes involved in representing a discrete system of particle as a continuum (see, for instance, Drew, 1983; Drew and Segal, 1971). The particle-phase viscous effects have been investigated by many previous investigators (see Gidaspow, 1986; Tsuo and Gidaspow, 1990; Gadiraju et al., 1991; Chamkha and Peddieson, 1994). Also, the particles are assumed to be dragged along by the fluid and, therefore, have no analog of pressure.

Equation (2*g*) assumes that the fluid phase is treated as an ideal gas. This equation is needed to render the problem determinant. The hydrodynamic and thermal coupling between the phases is accounted for by the interphase drag force and the interphase heat transfer. Other interphase mechanisms such as the virtual mass force (Zuber, 1964), the shear lift force (Saffman, 1965), and the spin-lift force (Rubinow and Keller, 1961) are neglected compared to the drag force. This is feasible when the particle Reynolds number is assumed to be small (see, for instance, Apazidis, 1985) as is the case in the present work.

Nomenclature

C = fluid-phase skin-friction coefficient
c = fluid-phase specific heat at constant pressure
D_p = particle-phase diffusion coefficient
Ec = fluid-phase Eckert number
e_x, e_y = unit vectors in x and y directions, respectively
F = nondimensionalized fluid-phase tangential (horizontal) velocity
f = interphase force per unit volume acting on the particle phase
G = nondimensionalized fluid-phase transformed normal (vertical) velocity
H = nondimensionalized fluid-phase temperature
I = unit tensor
k = fluid-phase thermal conductivity
P = fluid-phase pressure
Pr = fluid-phase Prandtl number
Q = nondimensional fluid-phase density
Q_T = interphase heat transfer rate per unit volume to the particle phase
r, S_R = constants defined in Eq. (16)
q_w = wall heat transfer
R = ideal gas constant
Re = Reynolds number
S_f = fluid-phase source term
S_p = particle-phase source term
S = particle-phase slip parameter
t_o = nondimensionalized fluid-phase wall temperature
T = fluid-phase temperature
u = x-component of velocity
U_∞ = free-stream velocity
v = y-component of velocity
V = fluid-phase velocity vector
x, y = Cartesian coordinate variables
β = viscosity ratio
δ = particle-phase inverse Schmidt's number
γ = specific heat ratio
Δ = fluid-phase displacement thickness
η = transformed normal (vertical) coordinate
Γ = fluid-phase viscosity coefficient
κ = particle mass loading ratio
μ = fluid-phase viscosity coefficient
ρ = fluid-phase density
σ = fluid-phase stress tensor
τ^* = wall shear stress
τ_T = temperature relaxation time
τ_v = momentum relaxation time
ω = power index for viscosity relation
ξ = transformed tangential (horizontal) coordinate
∇ = gradient operator
∇^2 = Laplacian operator

Subscripts

∞ = free stream
p = particle phase

Superscripts

T = transpose of a second-order tensor

The viscosity-temperature relation for the gas phase is assumed to be

$$\frac{\mu}{\mu_\infty} = \left(\frac{T}{T_\infty}\right)^{\omega} \quad (0.5 \le \omega \le 1.0). \tag{3}$$

This equation is similar to that employed by Wang and Glass (1988). Singleton (1965) employed $\omega = 0.5$ in his work on this problem.

In the absence of a fundamental knowledge on how the particle-phase diffusivity and dynamic viscosity vary with temperature and because the particle phase is treated as a continuum, it will be assumed that

$$\frac{D_p}{D_{p\infty}} = \left(\frac{T_p}{T_\infty}\right)^{\omega_p}, \frac{\mu_p}{\mu_{p\infty}} = \left(\frac{T_p}{T_\infty}\right)^{\omega_p} \quad (0.5 \le \omega_p \le 1.0) \quad (4a,b)$$

where ω_p is a particle-phase power index coefficient.

An appropriate set of boundary conditions suggested by the physics of the problem can be written as

$$u(x, 0) = 0,\ v(x, 0) = 0,\ T(x, 0) = T_W,$$

$$u_p(x, 0) = S\frac{\partial u_p}{\partial y}(x, 0),$$

$$v_p(x, 0) = 0,\ \frac{\partial \rho_p}{\partial y}(x, 0) = 0 \tag{5a–f}$$

$$u(x, \infty) = U_\infty,\ u_p(x, \infty) = U_\infty,$$

$$v_p(x, \infty) = v(x, \infty),\ T(x, \infty) = T_\infty$$

$$T_p(x, \infty) = T_\infty,\ \rho(x, \infty) = \rho_\infty,\ \rho_p(x, \infty) = \kappa\rho_\infty. \quad (5g–l)$$

Equations (5*a–c*) indicate that the fluid phase exhibits a no-slip condition at the plate surface, has no normal velocity at the wall, and is maintained at a uniform temperature, T_w, at the wall, respectively. The exact form of boundary conditions to be satisfied by a particle phase at the wall is unknown at present. There is, however, certain evidence that the particle phase experiences some slip near a boundary. Because of this and since the particle phase may resemble a rarefied gas, a boundary condition similar to that usually employed in rarefied gas dynamics is used in Eq. (5*d*). It is clear that this boundary condition allows for no slip when $S = 0$ and perfect slip when $S = \infty$. A similar form has been employed by Soo (1989). Equation (5*e*) indicates that there in normal velocity for the particle phase at the wall. Equation (5*f*) causes the particle-phase diffusivity effects to vanish at the plate. The rest of Eqs. (5) are matching conditions for both phases far above the plate and they indicate that both phases are in equilibrium with the free-stream conditions.

In the present work, a convenient set of modified Blasius transformations (similar to those employed previously by Chamkha and Peddieson, 1994) converts the tangential distance from being semi-infinite in $x(0 \le x < \infty)$ to finite in $\xi(0 \le \xi \le 1)$. The transformed equations eliminate the singularities associated with the leading edge of the plate and allows an exact solution at the leading edge of the plate ($\xi = 0$) (instead of assuming initial profiles of the dependent variables to start off the solution procedure as used by Wang and Glass, 1988). The set of transformations is as follows:

$$x = U_\infty\xi\tau_v/(1 - \xi),\ y = U_\infty\tau_v/\mathrm{Re}_\infty^{1/2}(2\xi/(1 - \xi))^{1/2}\eta$$

$$u = U_\infty F,\ v = U_\infty((1 - \xi)/(2\xi))^{1/2}(G + \eta F)/\mathrm{Re}_\infty^{1/2}$$

$$u_p = U_\infty F_p,\ v_p = U_\infty((1 - \xi)/(2\xi))^{1/2}(G_p + \eta F_p)/\mathrm{Re}_\infty^{1/2}$$

$$T = T_\infty H,\ T_p = T_\infty H_p,\ \rho = \rho_\infty Q,\ \rho_p = \kappa\rho_\infty Q_p,\ \mu_p = \mu_{p\infty}\Gamma_p$$

$$\mu = \mu_\infty\Gamma,\ \beta = \mu_{p\infty}/\mu_\infty,\ \delta = D_{p\infty}\rho_\infty/\mu_\infty,$$

$$\mathrm{Pr} = \mu c/k,\ \mathrm{Ec} = U_\infty^2/(cT_\infty)$$

$$\gamma = c/c_p,\ \mathrm{Re}_\infty = \rho_\infty U_\infty^2\tau_v/\mu_\infty. \tag{6}$$

Substituting Eqs. (6) (with $\kappa = 1$ following Wang and Glass, 1988) along with Eqs. (3) and (4) into Eqs. (1) and (2) transforms the problem to

$$\frac{\partial(QG)}{\partial\eta} + QF + 2\xi(1 - \xi)\frac{\partial(QF)}{\partial\xi} = 0 \tag{7}$$

$$\Gamma\frac{\partial^2 F}{\partial\eta^2} + \left(\frac{d\Gamma}{dH}\frac{\partial H}{\partial\eta} - QG\right)\frac{\partial F}{\partial\eta} - \frac{2\xi}{1 - \xi}\left((1 - \xi)^2 QF\frac{\partial F}{\partial\xi} - Q_p\Gamma(F_p - F)\right) = 0 \tag{8}$$

$$\Gamma\frac{\partial^2 H}{\partial\eta^2} + \left(\frac{d\Gamma}{dH}\frac{\partial H}{\partial\eta} - \mathrm{Pr}QG\right)\frac{\partial H}{\partial\eta} - 2\xi(1 - \xi)\,\mathrm{Pr}QF\frac{\partial H}{\partial\xi} + \mathrm{Pr}\,\mathrm{Ec}\Gamma\left(\frac{\partial F}{\partial\eta}\right)^2 + \left(\frac{2\xi}{1 - \xi}\right)\left(\mathrm{Pr}\,\mathrm{Ec}\Gamma Q_p(F_p - F)^2 + \frac{2\Gamma Q_p}{3}(H_p - H)\right) = 0 \tag{9}$$

$$QH = 1 \tag{10}$$

$$\delta D_p\frac{\partial^2 Q_p}{\partial\eta^2} + \left(\delta\frac{dD_p}{dH_p}\frac{\partial H_p}{\partial\eta} - G_p\right)\frac{\partial Q_p}{\partial\eta} - \left(F_p + \frac{\partial G_p}{\partial\eta}\right)Q_p - 2\xi(1 - \xi)\frac{\partial(Q_pF_p)}{\partial\xi} = 0 \tag{11}$$

$$\beta\Gamma_p\frac{\partial^2 F_p}{\partial\eta^2} + \left(\beta\frac{d\Gamma_p}{dH_p}\frac{\partial H_p}{\partial\eta} - Q_pG_p\right)\frac{\partial F_p}{\partial\eta} - \left(\frac{2\xi}{1 - \xi}\right)(\Gamma Q_p(F_p - F) + (1 - \xi)^2 Q_pF_p\frac{\partial F_p}{\partial\xi} = 0 \tag{12}$$

$$\beta\left(\Gamma_p\frac{\partial^2}{\partial\eta^2}(G_p + \eta F_p) + \frac{d\Gamma_p}{dH_p}\frac{\partial H_p}{\partial\eta}\frac{\partial}{\partial\eta}(G_p + \eta F_p)\right) - Q_pG_p\frac{\partial G_p}{\partial\eta} - \eta Q_pG_p\frac{\partial F_p}{\partial\eta} + \eta Q_pF_p^2 - \left(\frac{2\xi}{1 - \xi}\right)\left((1 - \xi)^2 Q_pF_p\frac{\partial}{\partial\xi}(G_p + \eta F_p) + \Gamma Q_p(G_p - G + \eta(F_p - F))\right) = 0 \tag{13}$$

$$Q_pG_p\frac{\partial H_p}{\partial\eta} + \left(\frac{2\xi}{1 - \xi}\right)\left((1 - \xi)^2 Q_pF_p\frac{\partial H_p}{\partial\xi} + \frac{2\Gamma\gamma}{3\,\mathrm{Pr}}Q_p(H_p - H)\right) - \beta\,\mathrm{Ec}\gamma\Gamma_p\left(\frac{\partial F_p}{\partial\eta}\right)^2 = 0. \tag{14}$$

Equations (7) through (14) represent the transformed boundary layer equations for a more generalized two-phase gas-solid model than that discussed by Marble (1970).

The dimensionless boundary conditions become

$$F(\xi, 0) = 0,\ G(\xi, 0) = 0,$$

$$F_p(\xi, 0) = S((1 - \xi)/(2\xi))^{1/2}\frac{\partial F_p}{\partial\eta}(\xi, 0)$$

$$H(\xi, 0) = t_0,\ G_p(\xi, 0) = 0,\ \frac{\partial Q_p}{\partial\eta}(\xi, 0) = 0,\ F(\xi, \infty) = 1$$

$$F_p(\xi, \infty) = 1,\ G_p(\xi, \infty) = G(\xi, \infty),\ H(\xi, \infty) = 1$$

$$H_p(\xi, \infty) = 1,\ Q(\xi, \infty) = 1,\ Q_p(\xi, \infty) = 1 \qquad (15)$$

where $t_0 = T_w/T_\infty$ is a dimensionless fluid-phase surface temperature.

In reality the particle-phase tangential velocity at the wall is controlled by many physical effects such as sliding friction, the nature of particle/surface collision, etc. It is not possible to model such effects with precision at present. Physically, a wall-slip condition should depend on the slip velocity between the fluid and the particle phases. It is known for this relaxation-type problem that the slip velocity is a function of the tangential distance ξ (see Soo, 1989). Therefore, to allow for a variety of particle-phase wall tangential velocity profiles, two wall-particle slip conditions will be investigated. The first condition is based on the assumption that the particle phase experiences a uniform slip action along the plate ($S = 1$) while in the second it is assumed that the wall-slip parameter S has the general form

$$S = S_R((1 - \xi)/\xi)^r \qquad (16)$$

(where S_R and r are constants). It can be seen that the form of Eq. (16) allows for perfect particulate slip taking $\xi = 0$, approaching a no-slip condition as determined by the values of S_R and r.

Of special practical significance for this problem are the fluid-phase displacement thickness δ^*, the particle-phase displacement thickness δ_p^*, the fluid-phase wall shear stress τ^*, the particle-phase wall shear stress τ_p^*, and the wall heat transfer coefficient q^*. These physical parameters are defined in dimensional form as

$$\delta^* = \int_0^\infty \left(1 - \frac{\rho u}{\rho_\infty u_\infty}\right) dy,\ \delta_p^* = \int_0^\infty \left(1 - \frac{\rho_p u_p}{\rho_{p\infty} u_\infty}\right) dy$$

$$\tau^* = \mu \frac{\partial u}{\partial y}(x, 0),\ \tau_p^* = \mu_p \frac{\partial u_p}{\partial y}(x, 0)$$

$$q^* = k \frac{\partial T}{\partial y}(x, 0). \qquad (17)$$

Substituting the dimensionless parameters in Eqs. (6) into Eqs. (17) produces the following dimensionless displacement thicknesses for the fluid and particle phases Δ and Δ_p, the skin-friction coefficients for the fluid and particle phases C and C_p, and the dimensionless wall heat transfer coefficient q_w.

$$\Delta(\xi) = \int_0^\infty (1 - QF)d\eta,\ \Delta_p(\xi) = \int_0^\infty (1 - Q_pF_p)d\eta,$$

$$C(\xi) = \Gamma(\xi, 0) \frac{\partial F}{\partial \eta}(\xi, 0)$$

$$C_p(\xi) = \beta\Gamma_p(\xi, 0) \frac{\partial F_p}{\partial \eta}(\xi, 0),$$

$$q_w(\xi) = \frac{\Gamma(\xi, 0)}{\mathrm{Ec\ Pr}} \frac{\partial H}{\partial \eta}(\xi, 0) \qquad (18)$$

Results and Discussion

Equations (7) through (14) are obviously nonlinear and, unfortunately, exhibit no closed-form or similar solution subject to Eqs. (15). They, therefore, must be solved numerically. The tridiagonal, implicit, iterative, finite difference method discussed by Blottner (1970) and Patankar (1980), which is similar to that used by Wang and Glass (1988), has proven to be successful in the solution of boundary layer problems. For this reason, it is adopted in the present work.

All first-order derivatives with respect to ξ are represented by three-point backward difference formulas. All second-order differential equations in η are discretized using a three-point central difference quotient while all first-order differential equations in η are discretized using the trapezoidal rule. The computational domain was divided into 1001 nodes in the ξ-direction and 195 nodes in the η-direction. Since it is expected that most changes in the boundary layer occur in the vicinity of the wall, variable step-sizes in η are utilized with $\Delta\eta_1 = 0.001$ and a growth factor of 1.03. Also, constant small step-sizes in ξ with $\Delta\xi = 0.001$ are used. The governing equations are then converted into sets of linear tridiagonal algebraic equations which are solved by the Thomas algorithm (see Blottner, 1970) at each iteration. The convergence criterion required that the difference between the current and the previous iterations be 10^{-5}. It should be mentioned that many numerical experimentations were performed by altering the step-sizes in both directions to ensure accuracy of the results and to assess grid independence. For example, when $\Delta\eta_1$ was set to 0.01 instead 0.001, an average error of about eight percent was observed in the results with the maximum error being close to $\xi = 1$. Also, when $\Delta\eta_1$ was equated to 0.0001 no significant changes of results were observed. For this reason $\Delta\eta_1 = 0.001$ was chosen and employed in producing the numerical results. The flow and heat transfer parameter are not as sensitive to $\Delta\xi$ as they are sensitive to $\Delta\eta_1$. For this reason, a constant step-size was used in the ξ-direction. The sensitivity analysis of the results to changes in $\Delta\xi$ was also performed. For instance, when $\Delta\xi$ was set to 0.01, an average deviation of five percent from the results with $\Delta\xi = 0.001$. Smaller values of $\Delta\xi$ than 0.001 produced no changes in the results and, therefore, $\Delta\xi$ was set to 0.001 in all the produced results. As far as the convergence criterion is concerned, two types were tried. One was based on the percentage error between the previous and the current iterations and the other was based on their difference. Since we are not dealing with very small numbers, the convergence criterion based on the difference between the previous and current iterations was employed in the present study. No convergence problems were encountered even with the small value of 10^{-5} used in this work. Equations (7) through (14) were solved for G, F, H, Q, Q_p, F_p, G_p, and H_p, respectively. Many results were obtained throughout the course of this work. A representative set is presented in Figs. 1 through 23 to show the effects of the physical parameters on the solutions. In all of the results to be reported subsequently, ω_p was equated to ω. This was done in order to minimize the number of figures after it was found that altering ω_p produced the same effects as that obtained by changing ω.

Nondiffusive Viscous Particle Phase. The governing equations and conditions for this special case are obtained by formally setting $\delta = 0$ in Eq. (11) and ignoring the boundary condition on Q_p at the wall. This special case has been solved previously by Chamkha (1996a). The major conclusion of his work was that a particle-free zone is predicted in which the particle-phase density

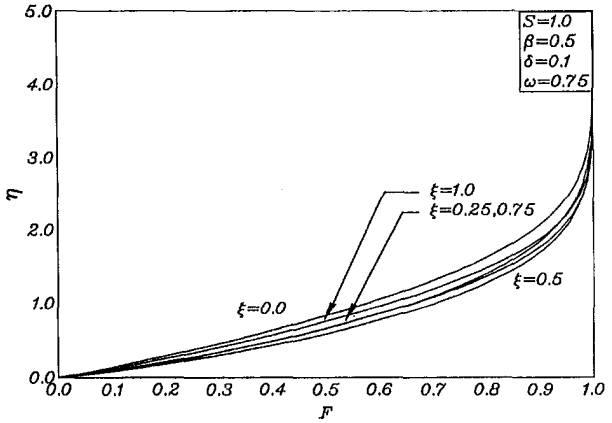

Fig. 1 Fluid-phase tangential velocity profiles

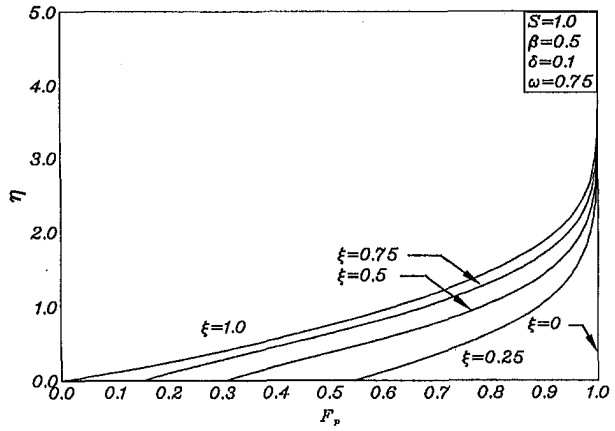

Fig. 2 Particle-phase tangential velocity profiles

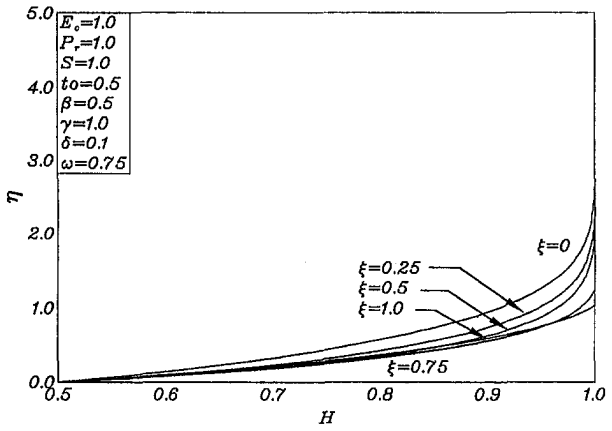

Fig. 5 Fluid-phase temperature profiles

at the wall vanished somewhere downstream of leading edge of the plate. In the present work, the particle-free zone phenomenon discussed by Chamkha (1996a) is reproduced as a limiting case as will be shown in Fig. 22.

If the vanishing of the particle-phase density at the wall represents a physical phenomenon, then the modified dusty-gas model employed by Chamkha (1996a) may be inadequate because the equations of this model are derived under the assumption that the entire space is occupied by both phases. Enhancements to the model which eliminates the existence of the particle-free zone is discussed later in this work.

Diffusive Inviscid Particle Phase. The mathematical model governing the present flow and heat transfer problem are obtained by setting $\beta = 0$ in Eqs. (12) through (14) and ignoring the third boundary condition given in Eq. (15). This case has also been considered by Chamkha (1998). It was found that qualitatively different results from those reported by Chamkha (1996a) were predicted. In fact, no particle-free zone was predicted. The influence of the particle-phase diffusivity was found to smooth off the sharp peaks in the wall particle-phase density distribution obtained for the case of $\beta = 0$ and $\delta = 0$. Therefore, it can be concluded from this and the previous case that a small change in the mathematical model can produce great changes in the predictions. Validation of this case with the present work is shown in Figs. 16 and 17.

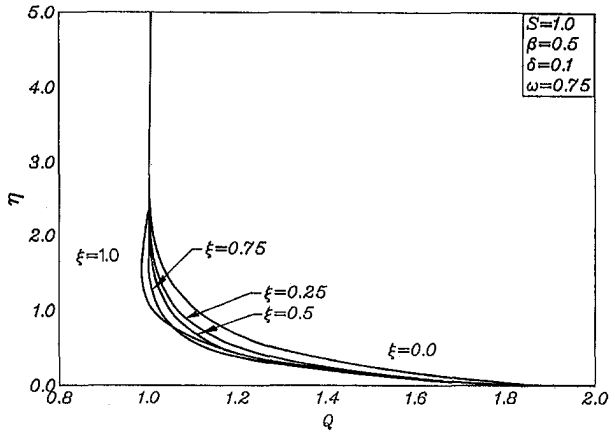

Fig. 3 Fluid-phase density profiles

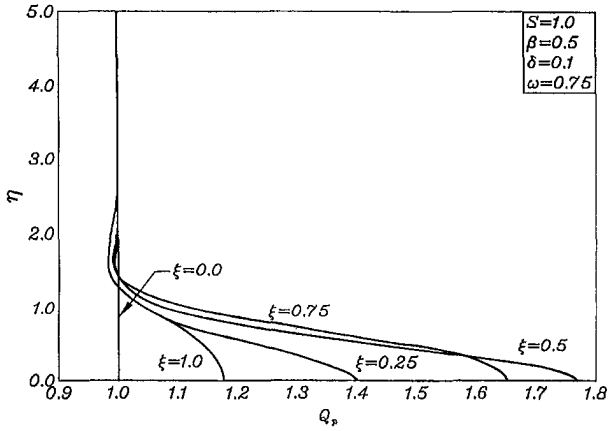

Fig. 4 Particle-phase density profiles

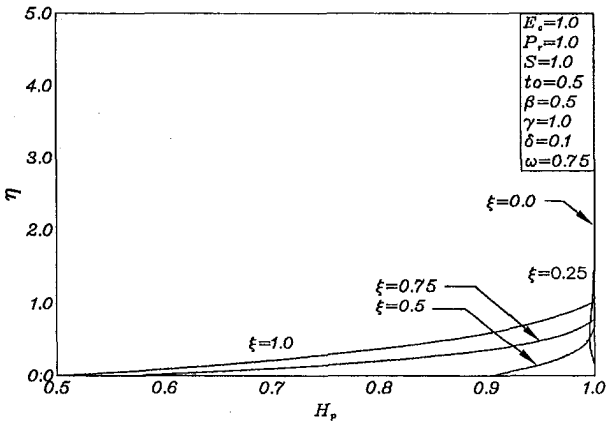

Fig. 6 Particle-phase temperature profiles

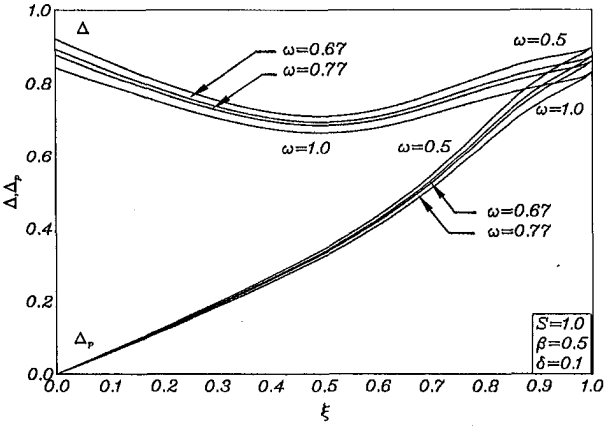

Fig. 7 Fluid and particle-phase displacement thicknesses profiles

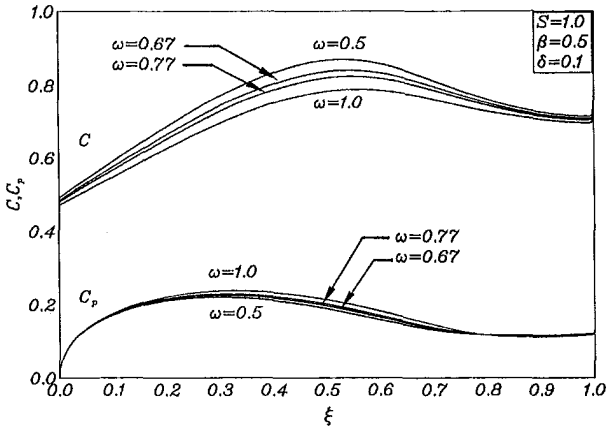

Fig. 8 Fluid and particle-phase skin friction coefficients profiles

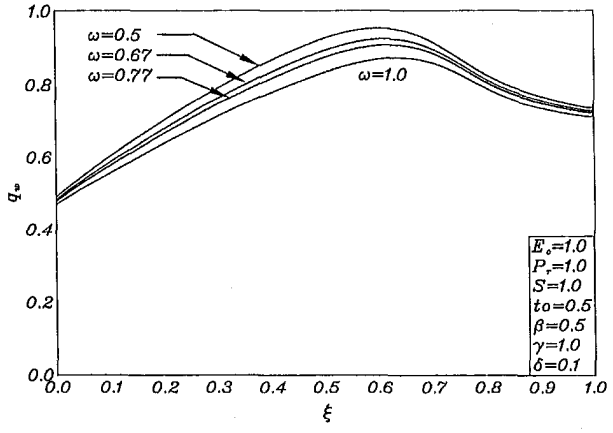

Fig. 11 Wall heat transfer coefficient profiles

Diffusive and Viscous Particle Phase. In this section the combined effects of particulate diffusivity and viscosity on the flow and heat transfer aspects of the problem under consideration are investigated. For this general case, the full equations given by Eqs. (7) through (14) subject to Eqs. (15) are solved numerically by the finite difference method previously discussed. Representative numerical results for this case are illustrated for both uniform and variable wall particle-phase slip conditions in Figs. 1 through 23. Figures 1 through 11 are for the uniform particle-phase wall slip ($S = 1$) while Figs. 12 through 23 are for the case of variable particle-phase wall slip according to Eq. (16) with $S_R = 50$ and $r = 1$.

Figures 1 through 6 present representative profiles for the fluid-phase tangential velocity F, particle-phase tangential velocity F_p, fluid-phase density Q, particle-phase density Q_p, fluid-phase temperature H, and the particle-phase temperature H_p at various locations along the plate, respectively. Equations (7) through (14) show that at $\xi = 0$, the motion of the fluid phase is uncoupled from the motion of the particle phase. This is called the frozen flow condition. In addition, it is observed that at $\xi = 1$ both phases move together with the same velocity and thermal conditions every where. This condition is called the equilibrium flow and thermal conditions. Figures 1 through 6 show the proper transition from

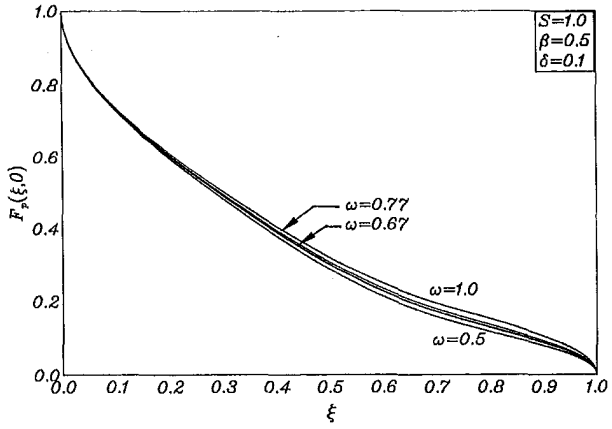

Fig. 9 Wall particle-phase tangential velocity profiles

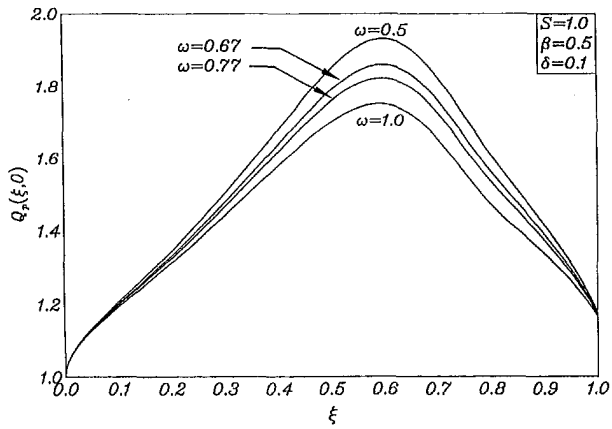

Fig. 10 Wall particle-phase density profiles

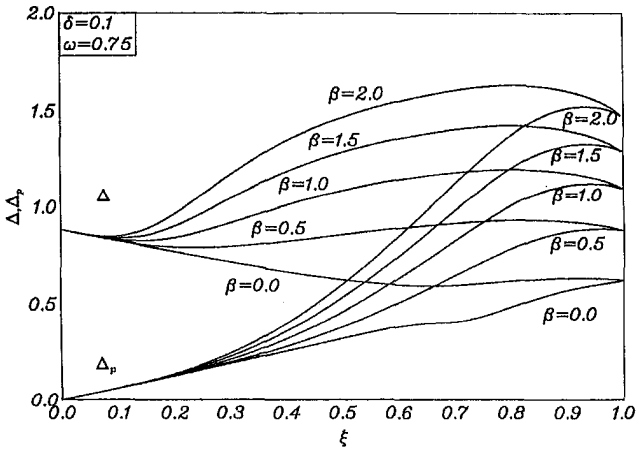

Fig. 12 Fluid and particle-phase displacement thicknesses profiles

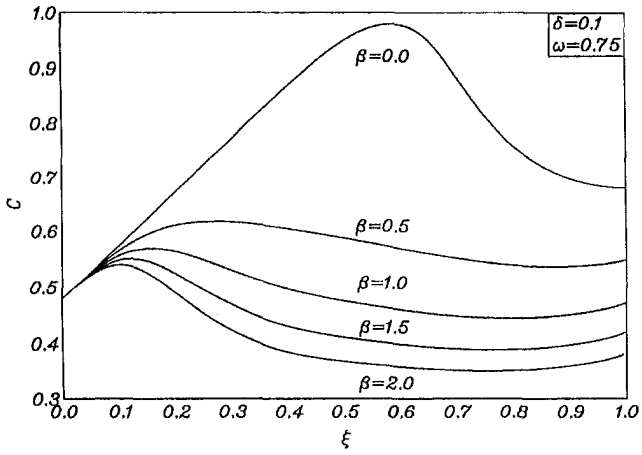

Fig. 13 Fluid-phase skin friction coefficient profiles

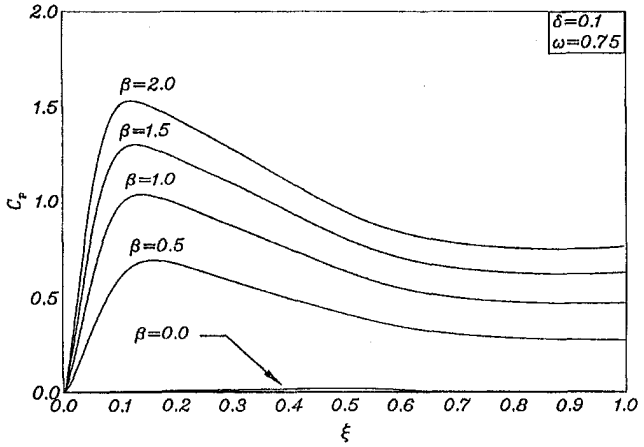

Fig. 14 Particle-phase skin friction coefficient profiles

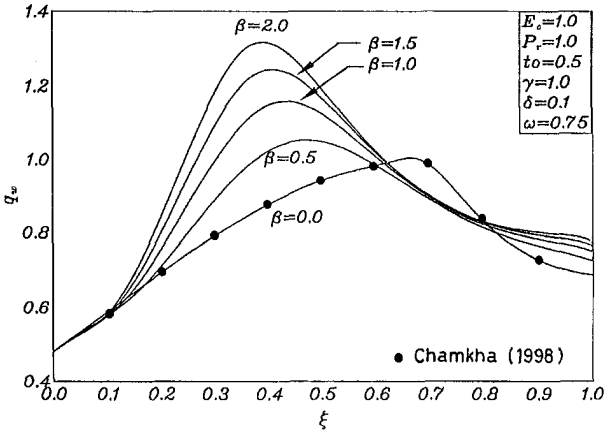

Fig. 17 Wall heat transfer coefficient profiles

frozen to equilibrium flow conditions. For large values of η both F and F_p approach unity while both the transformed normal velocities G and G_p (not shown here for brevity) approach $-\eta$. This is consistent with the definitions of the actual normal velocities v and v_p in Eqs. (6) since they must vanish at the edge of the boundary layer. The effect of the particle-phase wall slip on the profiles of F_p is apparent in Fig. 2 as it causes $F_p(\xi, 0)$ to decrease from unity (perfect slip) to zero (no slip). Figures 3 and 4 show that all deviations of Q and Q_p from uniformity are confined to a small region close to the plate surface where significant deviations from equilibrium exist. The development of the particle-phase wall temperature $H_p(\xi, 0)$ as the suspension moves from $\xi = 0$ to $\xi = 1$ and the thermal equilibrium condition where the profile of H_p is the same as that of H at $\xi = 1$ are apparent from Figs. 5 and 6.

Figures 7 and 8 illustrate the development of the displacement thicknesses (Δ and Δ_p) and the skin-friction coefficients (C and C_p) for both the fluid and particle phases along the plate tangential distance ξ for various fluid-phase power index coefficients ω. Physically speaking, at the leading edge of the plate, a frozen flow condition exists where both phases move independently. As a result, the drag force between the phases is maximum. As the flow

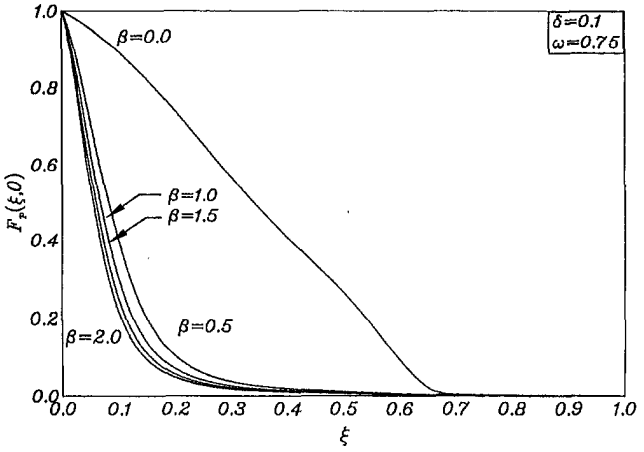

Fig. 15 Wall particle-phase tangential velocity profiles

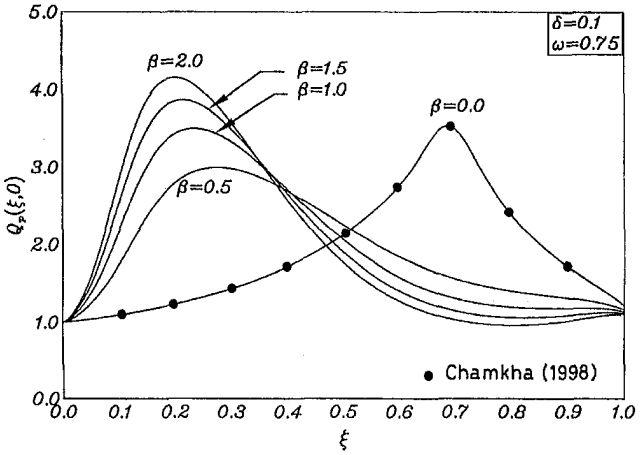

Fig. 16 Wall particle-phase density profiles

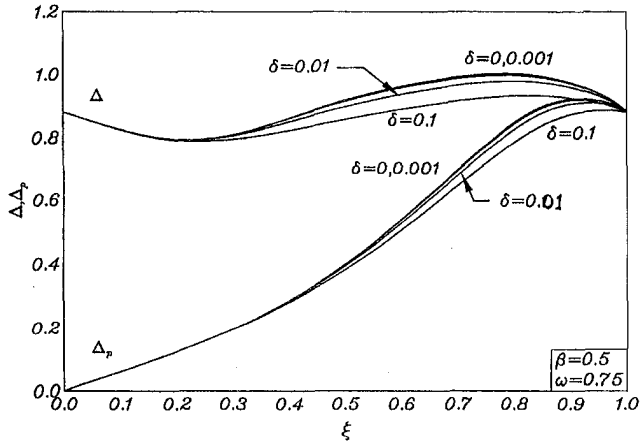

Fig. 18 Fluid and particle-phase displacement thicknesses profiles

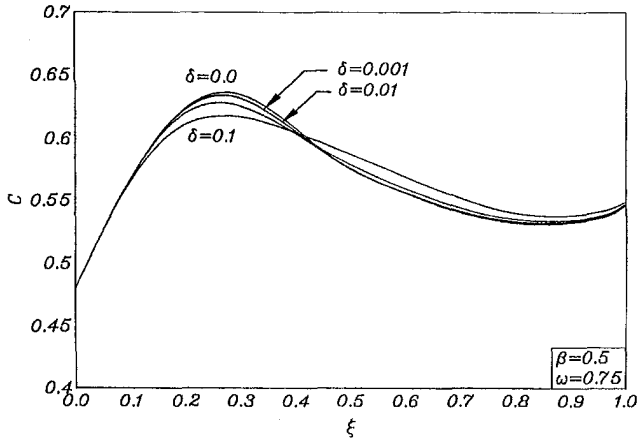

Fig. 19 Fluid-phase skin friction coefficient profiles

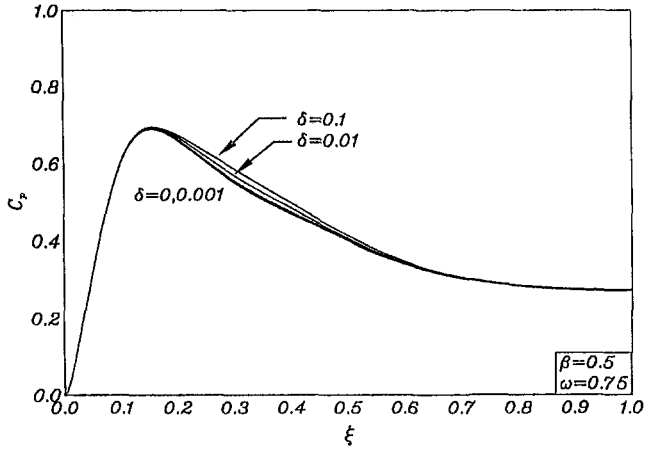

Fig. 20 Particle-phase skin friction coefficient profiles

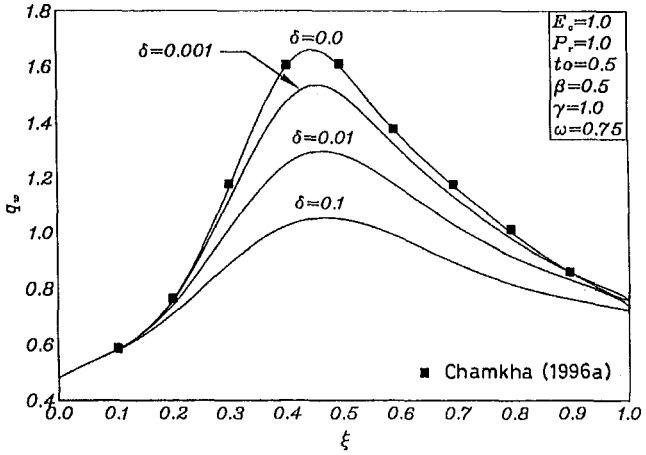

Fig. 23 Wall heat transfer coefficient profiles

moves downstream of the plate's leading edge, the momentum exchange mechanism through the drag force increases causing Δ to decrease and Δ_p to increase until an equilibrium condition where both the fluid and the particle phases move together is reached at $\xi = 1$. However, the values of C and C_p tend to increase to a peak and then decrease to their corresponding equilibrium values. The nonzero or finite values of Δ at the leading edge of the plate ($\xi = 0$) seems contrary to conventional single-phase flow over a semi-infinite flat plate (the Blasius problem). However, with the use of the modified Blasius transformations (Eqs. (6)) for the two-phase flow situation, the obtained solutions of F and Q at $\xi = 0$ are not uniform as seen from Figs. 1 and 3 as required for a vanishing value of Δ (see Eq. (18)). Therefore, it is expected that Δ takes on a nonzero or finite value at $\xi = 0$. These behaviors for Δ, Δ_p, C, and C_p are clearly depicted in Figs. 7 and 8. Furthermore, as the fluid-phase power index coefficient ω increases, moderate reductions in Δ, Δ_p, and C and slight increases in C_p are predicted as seen in Figs. 7 and 8.

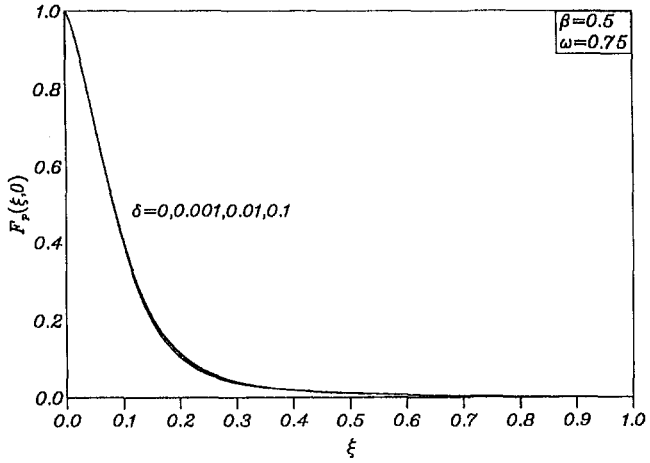

Fig. 21 Wall particle-phase tangential velocity profiles

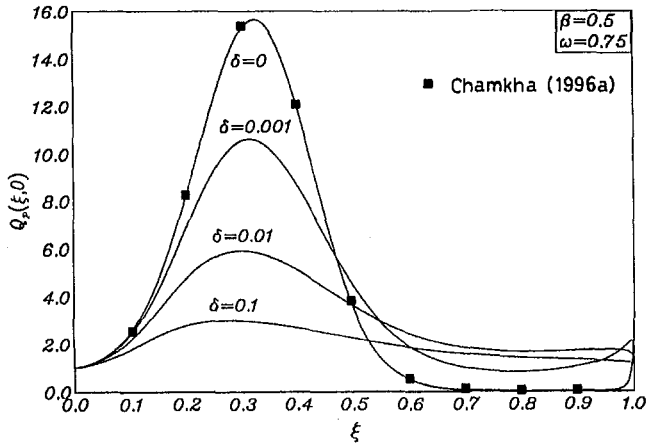

Fig. 22 Wall particle-phase density profiles

Figures 9 and 10 present representative profiles for the particle-phase tangential velocity and density at the wall for various values of the fluid-phase power index coefficient ω. At $\xi = 0$, the particle phase experiences a perfect slip condition at the wall with a uniform density distribution. As ξ increases and the interaction between the phases takes place, the drag force begins to decrease. As a result, the particle-phase wall tangential velocity $F_p(\xi, 0)$ starts to decrease and the particle-phase wall density $Q_p(\xi, 0)$ starts to increase until it reaches a maximum value in the vicinity of $\xi = 0.6$ after which it decreases until it reaches a quasi-equilibrium condition at $\xi = 0.1$. This type of behavior for $Q_p(\xi, 0)$ was predicted in analysis of the incompressible version of the present problem but there it became infinite (suggesting the presence of a singularity) when $F_p(\xi, 0)$ vanished (see, for instance, Osiptsov, 1980; Datta and Mishra, 1982; Chamkha and Peddieson, 1989). However, in the present analysis a continuous nonsingular solution exists throughout the computational domain. These behaviors in $F_p(\xi, 0)$ and $Q_p(\xi, 0)$ are clearly illustrated in Figs. 9 and 10, respectively. The effect of increasing ω is seen to increase $F_p(\xi, 0)$ slightly and to spread the particles away from the wall causing a significant reduction in the peak values of $Q_p(\xi, 0)$ as shown in Figs. 9 and 10.

In Fig. 11, the wall heat transfer coefficient q_w is presented along the plate for various values of ω. It is seen from this figure that q_w increases to a peak in the vicinity of $\xi = 0.6$ where $Q_p(\xi, 0)$ is maximum and then decreases to a limiting value at $\xi = 1$. It is also seen that as ω is increased q_w is decreased due to the corresponding decreases in $Q_p(\xi, 0)$. This suggests that the energy transfer between the phases increases as the density of the particles increases which, in turn, augments the wall heat transfer as depicted in Fig. 11.

Figures 12 through 14 depict the influence of β on Δ, Δ_p, C, C_p in the presence of a finite value of diffusivity ($\delta = 0.1$) respectively. At $\xi = 0$, the drag force between the phases is maximum and decreases as ξ increases until it vanishes at $\xi = 1$ where equilibrium exists. This momentum exchange causes Δ to decrease (which causes an increase in C) and Δ_p to increase until equilibrium at $\xi = 1$ is reached. However, as β increases, the effective viscosity of the mixture increases and causes a rapid increase in the values of Δ as the flow moves downstream towards equilibrium. Also, increasing β increases the domain of particle-phase viscous

effects causing Δ, Δ_p, and C_p to increase and C to decrease. These facts are clearly shown in Figs. 12 through 14. In addition, the distinctive peak in the values of C for $\beta = 0$ and $\delta = 0$ (inviscid nondiffusive particle phase discussed by Chamkha (1996a)) is still seen for the case where δ is included in the model. However, the effect of including δ in the model is seen to reduce the value of C as clearly shown in Fig. 13.

Figures 15 through 17 illustrate the distributions of the particle-phase tangential velocity and density at the wall and the wall heat transfer coefficient in the presence of particulate diffusivity ($\delta = 0.1$) along the plate for various values of the viscosity ratio β, respectively. It is seen from Fig. 15 that the region of large particulate wall slip is confined to the range $0 \leq \xi \leq 0.25$ for $\beta \neq 0$. As mentioned before, this range is controlled by the choice of the parameters S_R and r. Also, as discussed earlier, the presence of particulate diffusion in the mathematical model (with $\beta = 0$) introduces a smoothing effect which, in turn, causes significant reductions in the values of $Q_p(\xi, 0)$ and q_w. The presence of a particulate viscosity in the dusty-gas model (with $\delta = 0$) results in reductions in the peak values observed for $Q_p(\xi, 0)$ and q_w and causes the peaks to move upstream towards the plate's leading edge as β increases. However, a comparison of Figs. 16 and 17 with the results reported by Chamkha (1996a, 1998) shows that when both β and δ are finite, a particle-free zone does not exist in the entire region $0 \leq \xi \leq 1$. Also, there exists no catastrophic growth in the particle-phase density at the wall. This appears to be ensured by the presence of the particulate diffusivity. However, what appears to be different when the combined effects of δ and β are present in the model is that as β increases the values of $Q_p(\xi, 0)$ and q_w increase above what is predicted for $\beta = 0$. This is in sharp contrast with what is observed earlier (see Chamkha, 1996a). This behavior in q_w appears to be physically reasonable since as the particle viscous effects increase, the heat dissipation from the particle-particle interaction or particle-surface interaction is transferred to the carrier fluid through the interphase heat transfer mechanism. This, in turn, tends to increase the fluid-phase heat transfer to the wall. Therefore, it can be concluded that a dusty-gas model allowing for both inertial transport and diffusion of particles is capable of predicting results that are singularity-free and physically acceptable.

Figures 18 through 23 present the influence of δ on Δ, Δ_p, C, C_p, $F_p(\xi, 0)$, $Q_p(\xi, 0)$ in the presence of particulate viscous effects, respectively. These results compare qualitatively with those reported by Chamkha (1998) for $\beta = 0$. However, it is worth noticing the smoother transition of the values of $F_p(\xi, 0)$ shown in Fig. 21 from perfect slip at $\xi = 0$ to no-slip conditions downstream than those shown earlier by Chamkha (1998). Also, it can easily be seen from Fig. 22 that $Q_p(\xi, 0)$ vanishes in the vicinity of $\xi = 0.7$ for the case of $\delta = 0$ and $\beta \neq 0$ which is consistent with what is discussed before. Figures 22 and 23 illustrate clearly that, in the presence of particulate viscous effects, the particle-phase diffusivity effect is amplified since it causes more variations in the quantitative values of $Q_p(\xi, 0)$ and q_w than observed before for $\beta = 0$. Furthermore, Fig. 22 suggests that the presence of a particulate diffusivity in the dusty-gas model no matter how small is capable of removing the particle-free zone observed for cases where $\beta \neq 0$ and $\delta = 0$.

It should be mentioned that the results associated with $\beta = 0$ and $\delta = 0$ were put in terms of their primitive untransformed variables and compared with those reported by Wang and Glass (1988) and were found to be in good agreement. Furthermore, additional favorable comparisons were performed with the incompressible results reported by Chamkha and Peddieson (1989) and Chamkha (1994) for $\beta = 0$ and $\delta \neq 0$.

In the absence of reported experimental results on the problem considered in this paper, and inspite of the favorable comparisons made (which lend confidence in the numerical procedure), it is difficult to be certain that the phenomena predicted in this work and the work reported previously by Chamkha (1996a, 1998) are physically possible. This is difficult to evaluate because of the contrast that these results offer when a small change in the mathematical model occurs. Therefore, it is highly recommended that experimental investigation of this problem be undertaken. The present and the previously reported results (Chamkha 1996a, 1998) can serve as a stimulus for this investigation by identifying a particular phenomenon to be investigated.

Conclusion

A continuum dusty-gas model modified to include combined particle-phase diffusive viscous effects was employed in analyzing steady, compressible, laminar, boundary layer flow of a particulate suspension over a flat surface. The mathematical model included balance equations for mass, momentum, and energy for each phase where diffusive transport of thermal energy in the particle phase was neglected and where thermal and momentum exchange between the phases was specified in terms of relaxation time constants. Following the carrier fluid viscosity, the particle phase was assumed to have a general power-law viscosity-temperature and diffusivity-temperature relation. The governing equations were solved numerically using an implicit, iterative, finite difference method. A parametric study was performed to show the effects of the particle-phase viscosity and diffusivity. In contrast with the incompressible version of the flat-plate problem, it was found that a continuous solution existed throughout the computational domain. Other major predictions of the present work are summarized as follows: for a viscous nondiffusive particle phase a particle-free zone is formed at the plate surface; for a diffusive nonviscous particle phase a significant reduction in wall heat transfer and particle concentration at the plate surface is predicted. When both particle-phase diffusive and viscous effects were included in the dusty-gas model, singularity-free solutions were predicted and significant differences in wall particle-phase density concentrations and wall heat transfer with those of previous cases were observed. These various predictions could not be verified by experimental data due to the absence of such data at present. However, favorable comparisons with previously published results on special cases of this problem were made which gave confidence in the accuracy of the numerical method. It is hoped that the present results will be of use to environmental agencies in Kuwait and the Gulf countries in understanding the dynamics of dust storms, in validating computer routines and serve as a stimulus for experimental work on the present problem.

References

Apazidis, N., 1985, "On Two-Dimensional Laminar Flows of a Particulate Suspension in the Presence of Gravity Field," *Int. J. Multiphase Flow,* Vol. 11, pp. 657–698.

Blottner, F. G., 1970, "Finite-Difference Methods of Solution of the Boundary-Layer Equations," *AIAA Journal,* Vol. 8, pp. 193–205.

Chamkha, A. J., 1994, "Effects of Particulate Diffusion on the Thermal Flat Plate Boundary Layer of a Two-Phase Suspension," ASME JOURNAL OF HEAT TRANSFER, Vol. 116, pp. 236–239.

Chamkha, A. J., 1996a, "Compressible Dusty-Gas Boundary-Layer Flow Over a Flat Surface," ASME *Journal of Fluids Engineering,* Vol. 118, pp. 179–185.

Chamkha, A. J., 1996b, "Compressible Two-Phase Boundary-Layer Flow with Finite Particulate Volume Fraction," *International Journal of Engineering Science,* Vol. 34, pp. 1409–1422.

Chamkha, A. J., 1998, "Effects of Particulate Diffusion on the Compressible Boundary-Layer Flow of a Two-Phase Suspension Over a Horizontal Surface," ASME *Journal of Fluids Engineering,* Vol. 120, pp. 146–151.

Chamkha, A. J., and Peddieson, J., 1989, "Boundary-Layer Flow of a Particle-Fluid Suspension Past a Flat Plate," *Developments in Mechanics,* Vol. 15, pp. 315–316.

Chamkha, A. J., and Peddieson, J., 1992, "Singular Behavior in Boundary-Layer Flow of a Dusty Gas," *AIAA Journal,* Vol. 30, pp. 2966–2968.

Chamkha, A. J., and Peddieson, J., 1994, "Boundary-Layer Theory of a Particulate Suspension with Finite Volume Fraction," ASME *Journal of Fluids Engineering,* Vol. 116, pp. 147–153.

Datta, N., and Mishra, S. K., 1982, "Boundary Layer Flow if a Dusty Fluid Over a Semi-Infinite Flat Plate," *Acta Mechanica,* Vol. 42, pp. 71–83.

Drew, D. A., 1983, "Mathematical Modeling of Two-phase Flow," *Annual Review of Fluid Mechanics,* Vol. 15, pp. 261–291.

Drew, D. A., and Segal, L. A., 1971, "Analysis of Fluidized Beds and Foams Using Averaged Equations," *Studies in Applied Mathematics,* Vol. 50, pp. 233–252.

Gadiraju, M., et al., 1992, "Exact Solutions for Two-Phase Vertical Pipe Flow," *Mechanics Research Communications,* Vol. 19, pp. 7–13.

Gidaspow, D., 1986, "Hydrodynamics of Fluidization and Heat Transfer: Super Computer Modeling," ASME *Applied Mechanics Reviews,* Vol. 39, pp. 1–23.

Kuerti, G., 1951, "The Laminar Boundary Layer in Compressible Flow," *Advances in Appl. Mech., II,* pp. 21–92.

Marble, F. E., 1970, "Dynamics of Dusty Gases," *Annual Review of Fluid Mechanics,* Vol. 2, pp. 297–446.

Osiptsov, A. N., 1980, "Structure of the Laminar Boundary Layer of a Disperse Medium on a Flat Plate," *Fluid Dynamics,* Vol. 15, pp. 512–517.

Patankar, S. V., 1980, *Numerical Heat Transfer and Fluid Flow,* McGraw-Hill, New York.

Prabha, S., and Jain, A. C., 1980, "On the Use of Compatibility Conditions in the Solution of Gas Particulate Boundary Layer Equations," *Applied Scientific Research,* Vol. 36, pp. 81–91.

Rubinow, S. I., and Keller, J. B., 1961, "The Transverse Force on a Spinning Sphere Moving in a Viscous Fluid," *Journal of Fluid Mechanics,* Vol. 11, pp. 447–459.

Saffman, P. G., 1965, "The Lift on a Small Sphere in a Slow Shear Flow," *Journal of Fluid Mechanics,* Vol. 22, pp. 385–400.

Singleton, R. E., 1965, "The Compressible Gas-Solid Particle Flow Over a Semi-Infinite Flat Plate," *ZAMP,* Vol. 16, pp. 421–449.

Soo, S. L., 1968, "Non-equilibrium Fluid Dynamics-Laminar Flow Over a Flat Plate," *ZAMP,* Vol. 19, pp. 545–563.

Soo, S. L., 1989, *Particulates and Continuum Multiphase Fluid Dynamics,* Hemisphere, New York, pp. 282, 292.

Stewartson, K., 1974, "Multistructured Boundary Layers on Flat Plates and Related Bodies," *Adv. Appl. Mech., 14,* Academic Press, New York, pp. 146–239.

Tsuo, Y. P., and Gidaspow, D., 1990, "Computation of Flow Patterns in Circulating Fluidized Beds," *AIChE Journal,* Vol. 36, pp. 888–896.

Wang, B. Y., and Glass, I. I., 1988, "Compressible Laminar Boundary-Layer Flows of a Dusty Gas Over a Semi-Infinite Flat Plate," *Journal of Fluid Mechanics,* Vol. 186, pp. 223–241.

Young, A. D., 1949, "Skin Friction in the Laminar Boundary Layer of a Compressible Flow," *Aero. Quart., I,* pp. 137–164.

Zuber, N., 1964, "On the Dispersed Two-Phase Flow in a Laminar Flow Region," *Chem. Engng Sci.,* Vol. 19, pp. 897–917.